AMERICAN SOCIETY FOR MICROBIOLOGY | Infection and Immunity®

MOLECULAR PATHOGENESIS

RocA Is an Accessory Protein to the Virulence-Regulating CovRS Two-Component System in Group A *Streptococcus*

Ira Jain, Eric W. Miller, Jessica L. Danger, Kathryn J. Pflughoeft, Paul Sumby

Department of Microbiology and Immunology, University of Nevada, Reno School of Medicine, Reno, Nevada, USA

ABSTRACT Regulating gene expression during infection is critical to the ability of pathogens to circumvent the immune response and cause disease. This is true for the group A *Streptococcus* (GAS), a pathogen that causes both invasive (e.g., necrotizing fasciitis) and noninvasive (e.g., pharyngitis) diseases. The control of virulence (CovRS) two-component system has a major role in regulating GAS virulence factor expression. The regulator of cov (RocA) protein, which is a predicted kinase, functions in an undetermined manner through CovRS to alter gene expression and reduce invasive disease virulence. Here, we show that the ectopic expression of a truncated RocA derivative, harboring the membrane-spanning domains but not the dimerization or HATPase domain, is sufficient to complement a *rocA* mutant strain. Coupled with a previous bioinformatic study, the data are consistent with RocA being a pseudokinase. RocA reduces the ability of serotype M1 GAS isolates to express capsule and to evade killing in human blood, phenotypes that are not observed for M3 or M18 GAS due to isolates of these serotypes naturally harboring mutant *rocA* alleles. In addition, we found that varying the RocA concentration attenuates the regulatory activity of Mg^{2+} and the antimicrobial peptide LL-37, which positively and negatively regulate CovS function, respectively. Thus, we propose that RocA is an accessory protein to the CovRS system that influences the ability of GAS to modulate gene expression in response to host factors. A model of how RocA interacts with CovRS, and of the regulatory consequences of such activity, is presented.

KEYWORDS *Streptococcus pyogenes*, bacterial pathogenesis, gene regulation

Received 1 May 2017 **Returned for modification** 26 May 2017 **Accepted** 5 August 2017

Accepted manuscript posted online 14 August 2017

Citation Jain I, Miller EW, Danger JL, Pflughoeft KJ, Sumby P. 2017. RocA is an accessory protein to the virulence-regulating CovRS two-component system in group A *Streptococcus*. Infect Immun 85:e00274-17. https://doi.org/10.1128/IAI.00274-17.

Editor Liise-anne Pirofski, Albert Einstein College of Medicine

Address correspondence to Paul Sumby, psumby@medicine.nevada.edu.

Bacterial pathogens often show intraspecies phenotypic variation, with differences in antibiotic resistance and disease potential being just two of several reported phenotypes (1, 2). In many cases, intraspecies phenotypic variation can in part be attributed to the variable presence of mobile genetic elements, such as the presence of a Shiga-like toxin-encoding bacteriophage in the enterohemorrhagic *Escherichia coli* pathotype (3) or the presence of bla_{OXA-23}-bearing plasmids or transposons in carbapenem-resistant *Acinetobacter baumannii* isolates (4, 5). An additional process that drives intraspecies phenotypic variation is the differential regulation of gene expression (6). For example, the hypervirulence of the USA300 lineage of *Staphylococcus aureus* isolates relative to those from the USA200 lineage is in part due to differences in the Agr regulatory system (7, 8), which is a major regulator of *S. aureus* virulence factor expression (9). The importance of identifying the mechanisms that control intraspecies variation is perhaps best highlighted by the negative impact that such variation can have on the diagnosis, treatment, and/or prevention of infections (10–12).

The group A *Streptococcus* (GAS) (*Streptococcus pyogenes*) is a strict human patho-

gen that colonizes the throat and skin and causes a variety of diseases ranging from mild (e.g., pharyngitis and impetigo) to severe (e.g., streptococcal toxic shock syndrome and necrotizing fasciitis) (13). Additionally, GAS exposure may trigger serious postinfection sequelae, including acute rheumatic fever or acute poststreptococcal glomerulonephritis (14). The remarkable diversity of GAS diseases can be traced to the ability of the pathogen to express a large repertoire of virulence factors, including adhesins, proteases, immunoprotective proteins, and superantigens (15, 16). The regulation of virulence factor expression in GAS occurs through the coordinated functions of 13 two-component regulatory systems (17), dozens of standalone transcription factors (18), and at least one small regulatory RNA (19).

GAS isolates are divided into more than 200 different serotypes based upon the sequence of the 5′ end of the M protein-encoding gene, *emm*. Importantly, epidemiological studies have uncovered nonrandom associations between certain GAS serotypes and disease phenotypes. For example, serotype M3 isolates are associated with particularly severe and lethal invasive infections (20), while serotype M18 isolates are associated with outbreaks of acute rheumatic fever (21). Recently, it was shown that M3 and M18 GAS isolates harbor serotype-specific mutations within the regulator of cov (*rocA*) gene (22–25). Working in the M3 GAS background, we found that this mutation enhances virulence in a mouse model of bacteremia, possibly providing a link to the association of M3 isolates with severe invasive infections (24). RocA shows sequence similarity to sensor kinases and hence is predicted to function by phosphorylating target proteins (26). Through transcriptome analysis, we determined that complementing *rocA* in an M3 isolate negatively regulated the expression of more than 50 genes, including more than a dozen that encode immunomodulatory virulence factors. These serotype-specific regulatory changes likely impact niche adaptation by M3 and M18 isolates, with a consequence of this being their observed skew in disease outcomes. We also discovered that the regulatory activity of RocA occurs via enhancement of the activity of the control of virulence (CovRS) two-component regulatory system, a system that negatively regulates the transcription of ~10% of GAS genes (27–34). Through unknown means, RocA enhances the abundance of the phosphorylated (active) form of the CovR response regulator, increasing repression of CovRS-regulated genes (24).

Here, we sought to characterize the RocA protein and to assess how it enhances the CovRS-mediated regulation of virulence factor expression. We found that RocA is a major regulator of virulence gene expression in serotype M1 GAS isolates, as assessed by transcriptomic analyses comparing parental, *rocA* deletion mutant, and complemented mutant derivatives. The regulation afforded by RocA attenuates the ability of M1 GAS to survive and proliferate in nonimmune whole human blood. We also found that a plasmid-expressed RocA variant consisting of only the membrane-spanning domains is sufficient to complement a *rocA* mutant strain, consistent with RocA indirectly enhancing CovR phosphorylation. Finally, we also discovered that the inhibition of CovS activity by the antimicrobial peptide LL-37 (35) does not occur in strains that lack or overexpress RocA, adding evidence that RocA functions by modulating CovS activity. The virulence consequences of functional or mutant *rocA* alleles are discussed, with particular reference to how the natural *rocA* mutation in M3 GAS isolates may influence the association of this serotype with severe invasive infections.

RESULTS

RocA negatively regulates the ability of serotype M1 GAS to express capsule and to survive in a blood bactericidal assay. Complementing the natural *rocA* mutations in clinical isolates of serotype M3 and M18 GAS reduces expression of the antiphagocytic hyaluronic acid (HA) capsule (22, 24). Thus, we initially set out to assess whether RocA controls capsule expression in a clinical isolate that is naturally *rocA*$^+$. For this purpose, we chose to work in the serotype M1 GAS background, a serotype that is highly prevalent in North America and Western Europe (36). To assess the contribution of RocA to M1 GAS capsule production, we compared the abundance of capsule produced by our representative parental M1 isolate, MGAS2221; a constructed *rocA* dele-

TABLE 1 Overview of the GAS strains used in this study

GAS strain	Description	Reference
MGAS2221	Representative M1 clinical isolate (*covRS*$^+$ *rocA*$^+$)	30
2221ΔrocA	MGAS2221 derivative in which *rocA* has been replaced with a spectinomycin resistance cassette	24
2221ΔrocA::rocA^{M1}	Complemented derivative of 2221ΔrocA in which the spectinomycin resistance cassette has been replaced with a functional *rocA* allele from serotype M1 GAS	24
MGAS2221(pDCBB)	MGAS2221 derivative containing the empty chloramphenicol-resistant vector pDCBB, a *phoZ*-less derivative of pDC123	32
MGAS2221(pRocA-M1)	MGAS2221 derivative containing the plasmid pRocA-M1, which is a pDCBB-based plasmid containing a functional *rocA* allele from M1 GAS	This study
2221ΔrocA(pDCBB)	2221Δ*rocA* derivative containing the empty chloramphenicol-resistant vector pDCBB	This study
2221ΔrocA(pRocA-M1)	2221ΔrocA derivative containing the plasmid pRocA-M1, which is a pDCBB-based plasmid containing a functional *rocA* allele from M1 GAS	This study
2221ΔcovS	MGAS2221 derivative that contains a mutant *covS* allele due to the deletion of a single nucleotide	30
MGAS10870	Representative M3 clinical isolate (*covRS*$^+$ *rocA* mutant)	46
10870(pDCBB)	MGAS10870 derivative containing the empty chloramphenicol-resistant vector pDCBB	57
10870(pRocA-M1)	MGAS10870 derivative containing the plasmid pRocA-M1, which is a pDCBB-based plasmid containing a functional *rocA* allele from M1 GAS	This study
10870(pRocA-M3)	MGAS10870 derivative containing the plasmid pRocA-M3, which is a pDCBB-based plasmid containing a nonfunctional *rocA* allele from M3 GAS	This study
10870(pRocA-M18)	MGAS10870 derivative containing the plasmid pRocA-M18, which is a pDCBB-based plasmid containing a nonfunctional *rocA* allele from M18 GAS	This study
10870(pRocA-M1$^{1–409}$)	MGAS10870 derivative containing the plasmid pRocA-M1$^{1–409}$, which is a pDCBB-based plasmid containing a truncated *rocA* allele from M1 GAS	This study
10870(pRocA-M1$^{1–328}$)	MGAS10870 derivative containing the plasmid pRocA-M1$^{1–328}$, which is a pDCBB-based plasmid containing a truncated *rocA* allele from M1 GAS	This study
10870(pRocA-M1$^{1–276}$)	MGAS10870 derivative containing the plasmid pRocA-M1$^{1–276}$, which is a pDCBB-based plasmid containing a truncated *rocA* allele from M1 GAS	This study
10870(pRocA-M1$^{1–221}$)	MGAS10870 derivative containing the plasmid pRocA-M1$^{1–221}$, which is a pDCBB-based plasmid containing a truncated *rocA* allele from M1 GAS	This study
10870(pRocA-M1$^{1–89}$)	MGAS10870 derivative containing the plasmid pRocA-M1$^{1–89}$, which is a pDCBB-based plasmid containing a truncated *rocA* allele from M1 GAS	This study

tion mutant derivative, 2221ΔrocA; and a chromosomally complemented 2221ΔrocA derivative, 2221ΔrocA::rocA^{M1} (Table 1). Deletion of *rocA* increased the production of capsule ~13-fold (Fig. 1A), a phenotype that was complemented by reintroduction of the *rocA* gene. Note that the alteration in capsule abundance between the tested

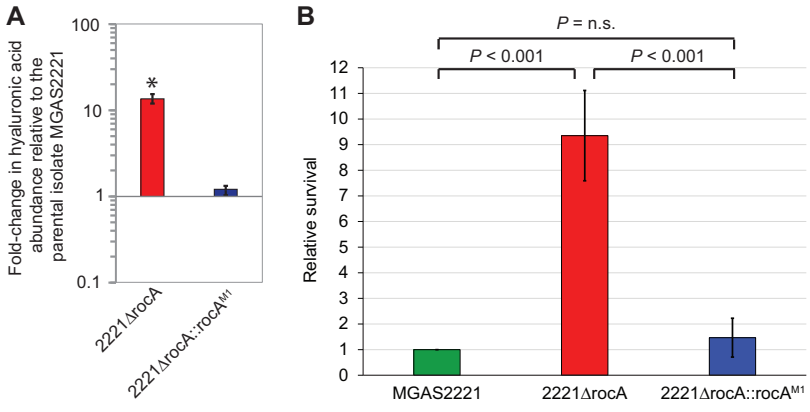

FIG 1 RocA negatively regulates capsule production and GAS survival in human blood in serotype M1 GAS. (A) The indicated GAS strains were analyzed for levels of the hyaluronic acid capsule. The experiment was performed twice, using duplicate cultures in each experiment, with mean (±standard deviation) values shown. The asterisk highlights statistical significance relative to the parental isolate (*t* test; $P < 0.01$). (B) Lancefield bactericidal assays. The indicated GAS strains were incubated with heparinized whole human blood, and percent survival was determined relative to the inoculum [(surviving CFU/initial CFU) × 100]. The experiment was performed in triplicate, with mean (±standard deviation) values shown. The *P* values shown were generated by *t* test (n.s., not significant).

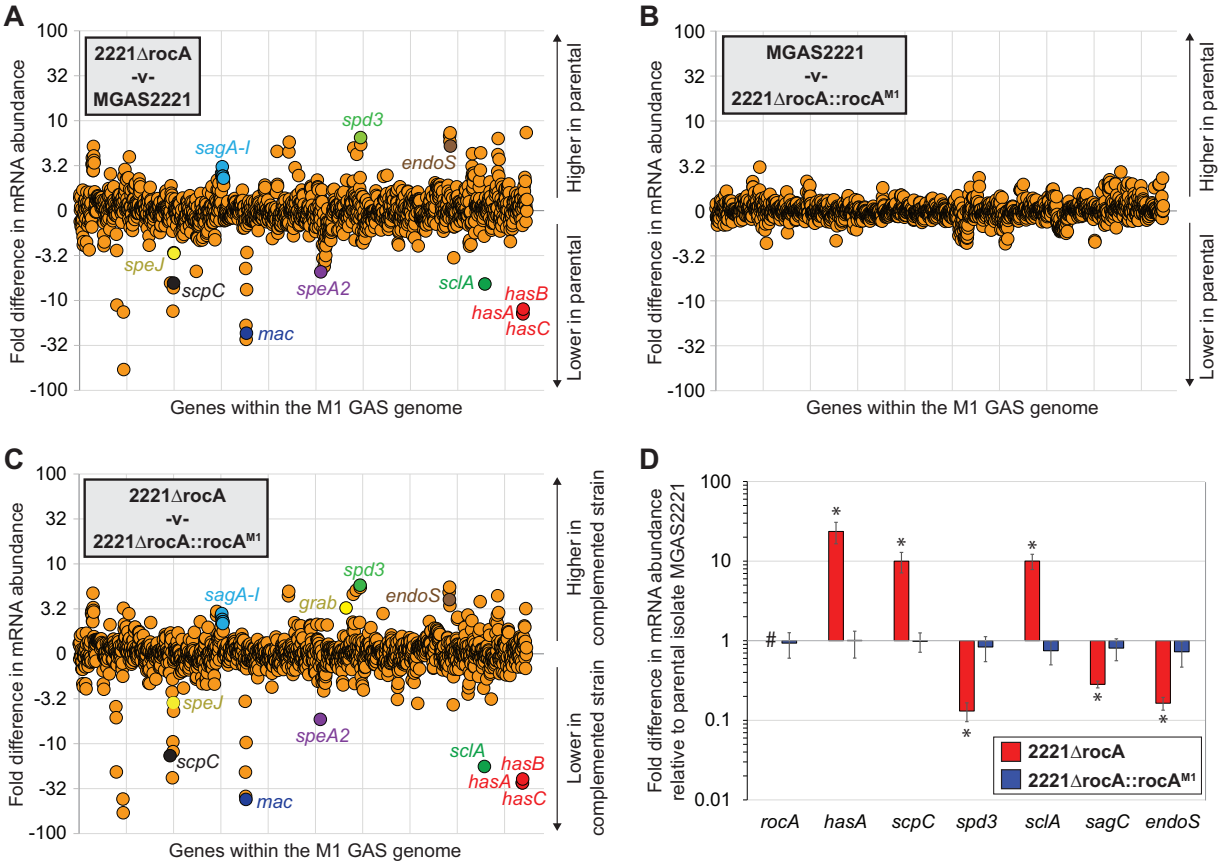

FIG 2 RocA reduces the abundance of multiple GAS transcripts. (A to C) Summary of RNA-seq data. Shown are pairwise comparisons of the transcriptomes between the parental M1 strain MGAS2221 and the *rocA* deletion mutant derivative 2221ΔrocA (A), between MGAS2221 and the complemented mutant derivative 2221ΔrocA::rocA^{M1} (B), and between 2221ΔrocA and 2221ΔrocA::rocA^{M1} (C). The relative expression levels of all the genes are graphed, with each represented by a circle. Select mRNAs of interest are colored and labeled. (D) TaqMan-based quantitative RT-PCR data confirming that RocA regulates the abundances of virulence factor-encoding mRNAs. The abundances of select transcripts were determined from duplicate exponential-phase GAS cultures run in triplicate, with the mean (±standard deviation) shown. The hash tag highlights the lack of *rocA* transcript in the *rocA* deletion mutant strain. The asterisks highlight statistical significance relative to the parental M1 isolate (*t* test; $P < 0.05$).

strains was not a consequence of differences in hyaluronidase activity (see Fig. S1 in the supplemental material).

Given that the capsule protects against neutrophil-mediated killing, we next assayed whether the regulatory activity afforded by RocA influenced the ability of M1 GAS to survive exposure to human blood. Bactericidal assays using heparinized nonimmune whole human blood determined that RocA reduced the survival of MGAS2221, and complemented mutant strain 2221ΔrocA::rocA^{M1}, relative to the *rocA* deletion mutant 2221ΔrocA (Fig. 1B). Thus, in serotype M1 GAS isolates, RocA negatively regulates survival in human blood and production of the antiphagocytic capsule.

RocA is a major negative regulator of GAS virulence factor expression. As serotype M3 isolates since at least the 1920s appear to be *rocA* mutants, it is possible that our previous RocA regulon data (24), generated in the M3 GAS background, may not accurately reflect the genes regulated by RocA in contemporary *rocA*$^+$ GAS isolates. Thus, to generate the first comprehensive data set of the RocA regulon for a naturally *rocA*$^+$ GAS isolate, we performed an RNA sequencing (RNA-seq)-based transcriptome analysis using M1 GAS. Comparing the transcriptomes between parental strain MGAS2221 and its *rocA* deletion mutant derivative, 2221ΔrocA, identified 47 transcripts that were statistically significantly different (Kal's Z test with false-discovery rate correction [37]; $P \leq 0.05$) at a 3-fold or greater level (Fig. 2A; see Table S1 in the supplemental material). Using the same parameters, only one transcript differed in the

MGAS2221 and 2221ΔrocA::rocA^{M1} comparison (Fig. 2B; see Table S2 in the supplemental material), while 42 transcripts differed in the 2221ΔrocA and 2221ΔrocA::rocA^{M1} comparison (Fig. 2C; see Table S3 in the supplemental material). While the majority of RocA-regulated genes overlapped data from our original M3 GAS transcriptome study (e.g., the capsule biosynthesis genes *hasABC*), others were identified as being RocA regulated for the first time (e.g., the *sag* operon encoding the hemolysin streptolysin S). The regulatory activity of RocA was confirmed for a subset of transcripts by TaqMan-based quantitative reverse transcription (RT)-PCR analysis (Fig. 2D). The data support RocA being a major regulator of gene expression in serotype M1 GAS.

Overexpressing RocA modifies the abundance of multiple virulence factor-encoding transcripts. To gain further insight into RocA function, we investigated whether the regulatory output of the protein could be modified upon overexpression. We tested this via RNA-seq, comparing derivatives of MGAS2221 and 2221ΔrocA containing the pDC123-derived vector pDCBB and a 2221ΔrocA derivative that overexpresses RocA from pDCBB [2221ΔrocA(pRocA-M1)] (Table 1). The RocA-overexpressing strain not only had a transcriptome distinct from that of the *rocA* deletion mutant strain (105 statistically significant transcripts differed by 3-fold or more) (see Fig. S2A and Table S6 in the supplemental material), but also from that of the parental strain (60 transcripts) (see Fig. S2B and Table S5). Of note, some transcripts were differentially regulated only upon RocA overexpression (that is, they were not differentially regulated between the parental and *rocA* deletion mutant strains), e.g., *slo*, encoding the hemolysin streptolysin O, and *sdaD2*, encoding a secreted DNase (see Fig. S2C and Table S4), while others were regulated to a greater extent upon RocA overexpression (e.g., *grab*, encoding the protease inhibitor-binding protein G-related α_2-macroglobulin, and *sse*, encoding a secreted esterase) (compare Fig. S2A and C). The differential regulation of select transcripts was verified by TaqMan-based quantitative RT-PCR analysis (see Fig. S2D). The data are consistent with RocA influencing GAS gene expression in a dose-dependent manner.

The truncated M3 GAS *rocA* allele complements a *rocA* mutant strain when expressed from a low-copy-number plasmid. Serotype M3 and M18 GAS isolates harbor serotype-specific null mutations within *rocA* (22, 24). The M3 *rocA* allele harbors a 1-bp deletion within a polynucleotide tract (going from 7 contiguous adenine nucleotides to 6), knocking the gene out of frame and resulting in a protein that is truncated within the C-terminal HATPase domain (Fig. 3A, blue asterisk) (23–25). The M18 *rocA* allele has a single nucleotide polymorphism (SNP) that introduces a premature stop codon early in the gene, resulting in a protein that is truncated after the third N-terminal transmembrane domain (Fig. 3A, green asterisk) (22). Previously, it was noted that the HATPase domain of RocA lacks several amino acids that are normally critical for kinase function, raising the possibility that RocA lacks kinase activity and hence is a pseudokinase (26). If RocA is a pseudokinase, we hypothesized that the RocA protein expressed by serotype M3 GAS, which is truncated within the HATPase domain, may retain residual activity and that this may be detected by overexpressing the protein in a *rocA* mutant strain background. To facilitate testing our hypothesis, we cloned the truncated M3 and M18 *rocA* alleles into vector pDCBB, creating plasmids pRocA-M3 and pRocA-M18. These plasmids and pRocA-M1, harboring the full-length serotype M1 *rocA* allele, were transformed into the naturally *rocA* mutant strain MGAS10870 (a serotype M3 GAS isolate) and compared with an empty-vector-containing derivative. The M1 and M3 *rocA* alleles were indistinguishable in their ability to complement MGAS10870, while the M18 *rocA* allele failed to complement (Fig. 3B). Thus, despite previous data showing that MGAS10870 and a *rocA* deletion mutant derivative have essentially identical transcriptomes (24), the M3 RocA protein retains residual activity, so it is capable of complementing a *rocA* mutant strain upon overexpression. The data also provide the first experimental support for RocA being a pseudokinase.

The DHp and HATPase domains of RocA are dispensable for regulatory activity. To identify which domains of RocA are essential or dispensable for regulatory activity, we

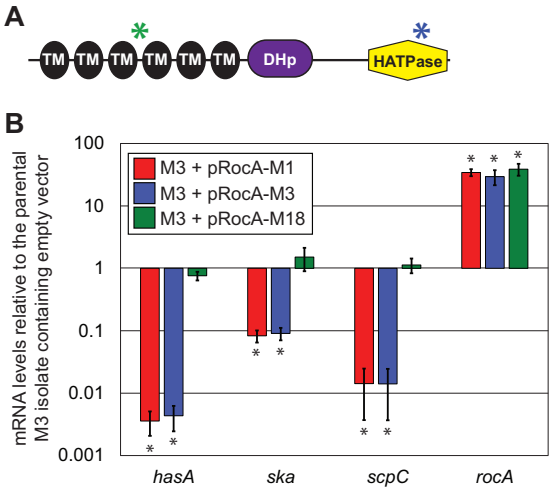

FIG 3 The full-length M1 and truncated M3 *rocA* alleles, but not the truncated M18 *rocA* allele, complement a *rocA* mutant when expressed from a multicopy plasmid. (A) Schematic of the RocA protein and of the locations of the truncations in the M3 (blue asterisk) and M18 (green asterisk) *rocA* alleles. RocA has six putative transmembrane domains (TM), a putative dimerization and histidine phosphotransfer domain (DHp), and a putative histidine kinase-like catalytic domain (HATPase). (B) TaqMan-based quantitative RT-PCR analysis to assay the abilities of the M1, M3, and M18 *rocA* alleles to complement the naturally *rocA* mutant M3 isolate MGAS10870. Shown are the averages (±standard deviations) of duplicate samples run in triplicate. The asterisks highlight statistical significance relative to the parental M3 isolate containing empty vector (*t* test; *, $P < 0.001$).

constructed a series of pRocA-M1 derivatives that express RocA with C-terminal truncations of increasing size (Fig. 4A). Note that the truncation in plasmid pRocA-M1$^{1-409}$ is identical to that present in the M3 *rocA* allele, while the truncation in pRocA-M1$^{1-89}$ is identical to that present in the M18 *rocA* allele. The plasmids were introduced into MGAS10870, and the ability of the shortened *rocA* alleles to complement was assayed by quantitative RT-PCR. With the exception of the plasmid harboring the largest *rocA* truncation, pRocA-M1$^{1-89}$, all the plasmids were able to complement the *rocA* mutation in MGAS10870 (Fig. 4B). Given that pRocA-M1$^{1-221}$ lacks the DHp and HATPase domains and yet is still able to complement, the data are consistent with the regulatory activity afforded by RocA residing within its membrane-spanning domains.

RocA is required for the regulation of CovRS activity by LL-37, but not by Mg^{2+}. Mg^{2+} and the amphipathic antimicrobial peptide LL-37 function as ligands for CovS (38, 39). At subinhibitory concentrations (e.g., concentrations at which no antibacterial action is observed), LL-37 binds to CovS and inhibits CovRS-mediated regulation, while Mg^{2+} has opposing activity and enhances CovRS-mediated regulation (35). Given our previous data showing that RocA directly or indirectly functions through CovRS (24), we reasoned that RocA may modify the ability of Mg^{2+} and/or LL-37 to regulate CovRS activity. To test our hypothesis, we grew MGAS2221 and derivatives 2221ΔcovS and 2221ΔrocA in standard Todd-Hewitt broth containing 0.2% yeast extract (THY broth), THY broth supplemented with 15 mM $MgCl_2$ (as a source of Mg^{2+}), and THY broth supplemented with 100 nM LL-37. Samples from the exponential phase of growth were analyzed by quantitative RT-PCR analysis of select CovRS-regulated genes. As expected, LL-37 reduced the CovRS-mediated repression of *slo*, *scpC* (encoding the chemokine protease SpyCEP), and *hasA* and enhanced repression of *grab* in MGAS2221 (Fig. 5A, red bars). In contrast, LL-37 had no regulatory activity in strain 2221ΔcovS (no difference between the dark-blue and blue bars in Fig. 5A), which was expected, given that LL-37 functions through CovS. Interestingly, LL-37 also had no regulatory activity in strain 2221ΔrocA (no difference between the dark-green and green bars in Fig. 5A). Thus, RocA is required for GAS to modulate the CovRS-mediated regulation of gene expression in response to the human antimicrobial peptide LL-37.

As Mg^{2+} enhances CovRS-mediated regulation while LL-37 inhibits it, the addition of $MgCl_2$ to the growth medium resulted in differential gene expression for strain

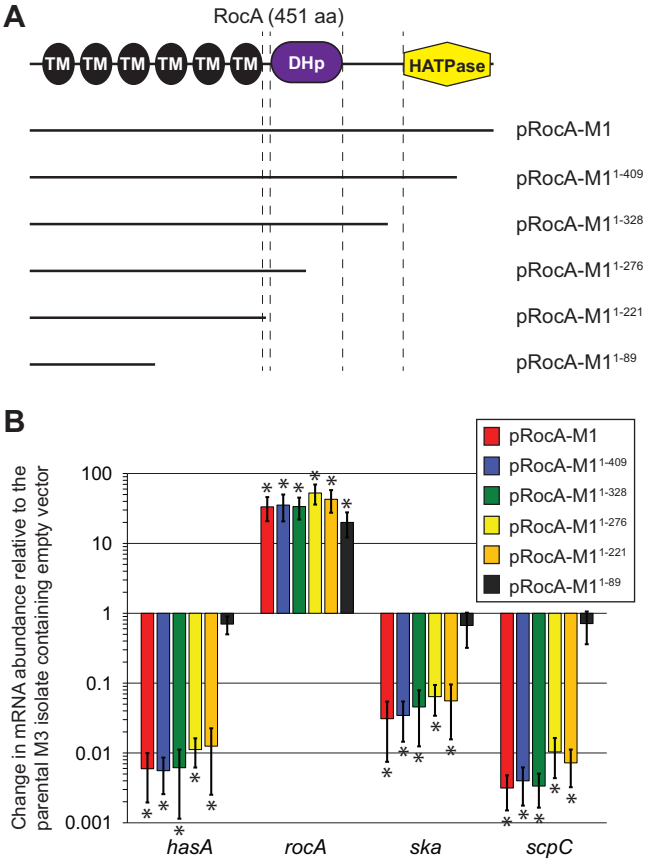

FIG 4 Overexpression of the membrane-spanning domains of RocA is sufficient for regulatory activity. (A) Schematic of the RocA protein and of the extent of RocA truncations within a series of constructed plasmids. (B) TaqMan-based quantitative RT-PCR analysis of *rocA* and select (*hasA*, *ska*, and *scpC*) RocA-regulated mRNA abundances. Derivatives of the naturally *rocA* mutant M3 isolate MGAS10870 containing the plasmids shown in panel A were compared to the same strain containing empty vector. Shown are the averages (±standard deviations) of triplicate samples run in duplicate. The asterisks highlight statistical significance relative to the parental M3 isolate containing empty vector (*t* test; *, $P < 0.001$).

MGAS2221 relative to the cultures grown in THY broth only or THY broth plus LL-37. More specifically, repression of *grab* was reduced and repression of *slo* was increased, while the repression of *scpC* and *hasA* was unchanged (Fig. 5A, pink bars) (see Discussion for our hypothesis as to why *scpC* and *hasA* were unchanged). With regard to strain 2221ΔcovS, the fact that $MgCl_2$ had no effect was expected, since Mg^{2+} is hypothesized to regulate CovRS activity by enhancing the kinase activity of CovS (no difference between the light- and dark-blue bars in Fig. 5A) (39). However, while 2221ΔcovS and 2221ΔrocA were essentially identical with regard to their inability to be regulated by LL-37, 2221ΔrocA appears to retain a partial ability to be regulated by Mg^{2+}. While the level of repression (*scpC* and *hasA*) or derepression (*grab*) by Mg^{2+} is not as dramatic as that observed in the parental strain, 2221ΔrocA nevertheless showed regulation (Fig. 5A, compare the light- and dark-green bars), highlighting the fact that Mg^{2+} maintains some regulatory activity in the absence of RocA. In summary, the data are consistent with the ability of the CovRS system to respond to host stimuli (LL-37 and Mg^{2+}) being at least partially dependent upon the presence of RocA.

Neither LL-37 nor Mg^{2+} influences GAS gene expression in a RocA overexpression strain. To further shed light on the involvement of RocA in the ability of LL-37 and Mg^{2+} to modulate GAS gene expression, we investigated the regulatory abilities of these factors in a RocA overexpression strain (MGAS2221, containing pRocA-M1). No significant difference in the abundance of select CovRS-regulated mRNAs was observed

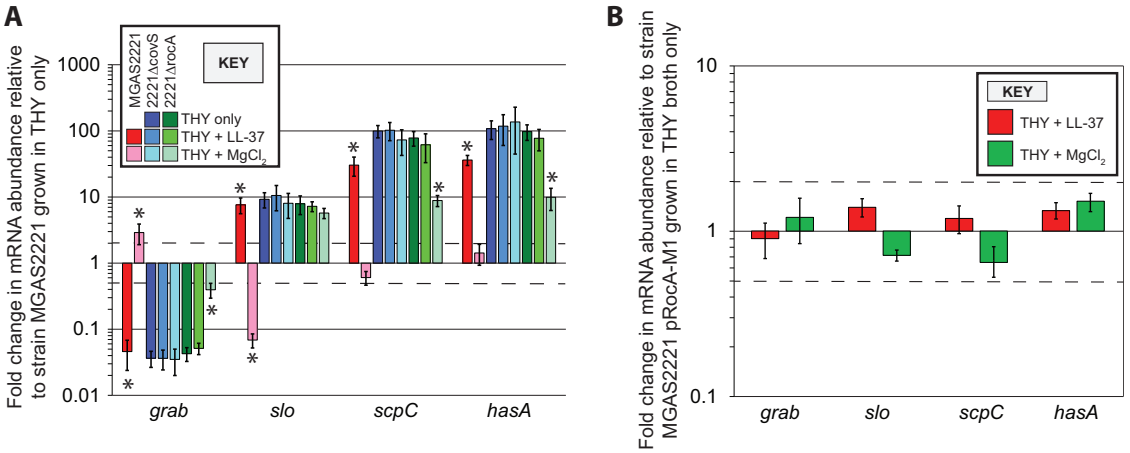

FIG 5 Inhibition of CovRS activity by the antimicrobial peptide LL-37 requires RocA. Shown are TaqMan-based quantitative RT-PCR analyses. GAS strains were grown to the exponential phase of growth in THY broth, THY broth containing 100 nM LL-37, and THY broth containing 15 mM $MgCl_2$. The strains analyzed were the parental M1 isolate MGAS2221 and derivatives 2221ΔcovS and 2221ΔrocA (A) and MGAS2221 containing the RocA-overexpressing plasmid pRocA-M1 (B). Relative transcript abundances between these strains and growth conditions were assayed. Shown are the averages (±standard deviations) of triplicate samples run in duplicate. The asterisks highlight statistical significance relative to the individual strains grown in THY broth only (*t* test; *, $P < 0.05$). The dashed lines indicate ±2-fold levels of regulation.

in the presence or absence of LL-37 or $MgCl_2$ (Fig. 5B). Thus, neither LL-37 nor Mg^{2+} is able to modulate CovRS system activity upon RocA overexpression.

DISCUSSION

Conclusions. Recently, it has become apparent that two-component systems from a diverse range of bacterial species require so-called accessory proteins for full regulatory activity (40, 41). In some instances (42, 43), the accessory proteins increase the number of stimuli capable of influencing the regulatory output of their associated two-component system, enabling a larger range of environments to be distinguished and a greater ability to tailor gene expression to each environment. Here, we discovered that RocA is a major regulator of virulence factor expression in serotype M1 GAS and that this regulatory activity reduces the ability of M1 GAS to survive and proliferate in human blood. We also generated data consistent with RocA being a pseudokinase rather than a kinase, as originally thought, and show that RocA enhances the ability of CovS to modulate its regulatory activity in the presence of LL-37 and Mg^{2+}. Thus, RocA is an accessory protein that, by working through CovRS, plays a key role in modulating GAS gene expression during infection.

Our model of how RocA interacts with the CovRS system, and the regulatory consequences of this interaction, is shown in Fig. 6. We propose that in the absence of RocA, CovS has only minimal kinase activity toward CovR, which is in accord with our previous data showing that the major form of CovR in a *rocA* mutant is the nonphosphorylated form (24). As nonphosphorylated CovR is for the most part considered inactive and unable to repress gene transcription from target promoters, this results in the enhanced expression of multiple genes, including several that encode immunomodulatory virulence factors (Fig. 2). The altered virulence factor expression profile due to *rocA* mutation results in an enhanced ability to cause invasive infections, as is evident from previous animal infection data (22, 24, 44) and also our blood bactericidal assays (Fig. 1B). We propose that CovS and RocA interact via their membrane-spanning domains, an interaction that enhances CovS kinase activity and, subsequently, the abundance of phosphorylated CovR (Fig. 6). High levels of phosphorylated CovR result in the repression of target gene transcription, producing a virulence factor expression profile suited to successfully causing noninvasive infections. One of several unanswered questions associated with our model is what is the benefit to GAS of having RocA

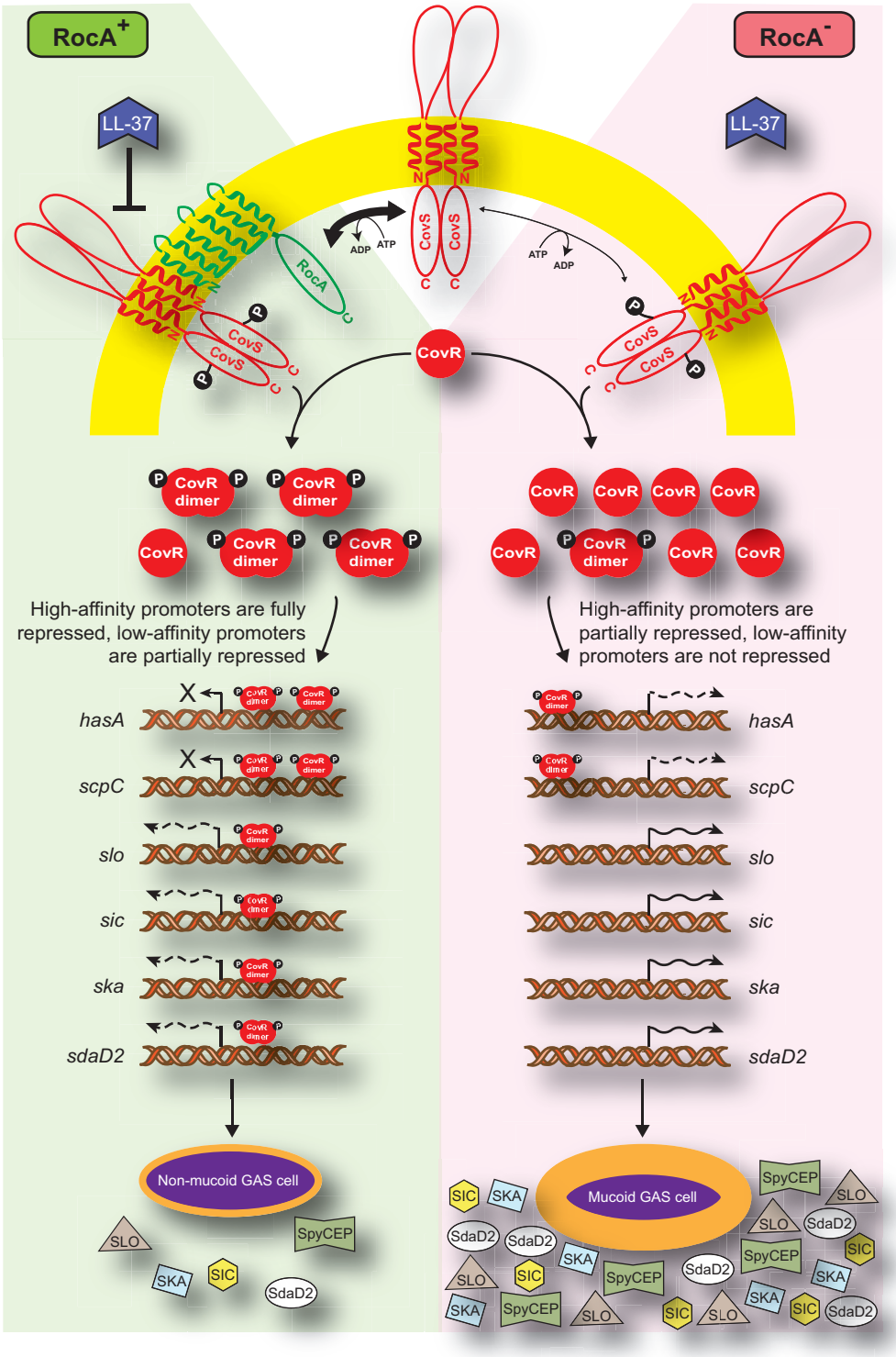

FIG 6 Model of how RocA enhances the activity of the CovRS system, leading to altered virulence factor expression and disease potential. The left side of the diagram (shaded green) displays what occurs in a *rocA*$^+$ GAS cell, while the right side (shaded pink) displays what occurs in a *rocA* mutant cell. RocA complexes with CovS and greatly enhances the CovS kinase activity, resulting in predominantly phosphorylated CovR protein (active), which can dimerize and repress gene expression. In the absence of RocA, CovS retains residual kinase activity, but the nonphosphorylated form of CovR (inactive) predominates. The antimicrobial peptide LL-37 inhibits the interaction between RocA and CovS, reducing CovRS-mediated activity, but has no regulatory effect in a *rocA* mutant strain. Given the high abundance of active CovR in a *rocA*$^+$ strain, the protein can bind to most CovR-repressible promoters, regardless of whether the promoters harbor high-affinity (e.g., *hasA* and *scpC*) or low-affinity (e.g., *slo*, *sic*, *ska*, and *sdaD2*) CovR-binding sites. The low abundance of active CovR in a *rocA*

(Continued on next page)

TABLE 2 Comparison of expression levels for select genes as determined by RNA-seq analysis[a]

Gene	Expression in:		
	2221ΔrocA + vector (no *rocA* mRNA)	MGAS2221 + vector (medium *rocA* mRNA levels)	2221ΔrocA(pRocA-M1) (high *rocA* mRNA levels)
hasA	1	0.025	0.020
slo	1	0.495	0.018
sic	1	0.428	0.022

[a]The data were extracted from the RNA-seq experiment shown in Fig. S2 in the supplemental material. Expression levels are displayed relative to those present in strain 2221ΔrocA + vector.

provide regulatory input into the CovRS system? We hypothesize that RocA recognizes as-yet-uncharacterized factors that control its ability to associate with CovS.

We found that LL-37 is unable to repress regulation by the CovRS system in the absence of RocA (Fig. 5A). Consistent with this finding are published data comparing the regulatory activities of LL-37 in five different GAS serotypes, with LL-37 having stronger activity in association with M1, M4, M5, and M29 GAS isolates than with an M3 isolate (38). As M1, M4, M5, and M29 GAS isolates are either known or thought to produce functional RocA while M3 GAS does not, this is most likely the molecular explanation behind the serotype-specific regulatory activity of LL-37. Why LL-37 has no regulatory activity in the absence of RocA (Fig. 5A) is unclear. One possibility is that RocA promotes the ability of CovS to bind LL-37 (35), while a second possibility is simply that CovS activity is already so highly attenuated in the absence of RocA that LL-37 has at best a negligible regulatory role. A third possibility, and the one that we favor, is that LL-37 regulates CovRS activity by inhibiting the abilities of RocA and CovS to interact (Fig. 6). Interestingly, LL-37 was also unable to inhibit CovS activity upon RocA overexpression (Fig. 5B). This could be explained by LL-37 and RocA competing for CovS binding, but experimentation to test this or other hypotheses is outside the limits of the present study.

An observation from our transcriptomic studies is that there appear to be gene-specific consequences to differing levels of RocA expression. For example, *hasA* is highly sensitive to regulation by RocA so that it is essentially maximally repressed in MGAS2221 relative to the derivative 2221ΔrocA, and hence, higher levels of RocA, such as are present in strain 2221ΔrocA(pRocA-M1), have little additional regulatory activity (Table 2). In contrast, *slo* and *sic* (encoding the streptococcal inhibitor of complement) mRNA levels are repressed only ~2-fold in MGAS2221 relative to 2221ΔrocA but ~50-fold in 2221ΔrocA(pRocA-M1) relative to 2221ΔrocA (Table 2). These data are consistent with a model in which phosphorylated CovR (CovR~P) binds to target promoters with differing affinities (45) and with *hasA*, but not *slo* or *sic*, having one of the highest-affinity promoters for CovR~P (Fig. 6). Thus, while the level of CovR~P is lower in the parental isolate than in the RocA-overexpressing strain, there is sufficient in the parental isolate to fully repress *hasA*. However, in part due to being sequestered by the *hasA* promoter, the level of CovR~P in the parental isolate is not sufficient to dramatically repress *slo* or *sic* transcription, while the increased level of CovR~P in the RocA-overexpressing strain is sufficient. This model is also supported by two observations from our study on the effects of Mg^{2+} on regulation by RocA, CovR, and CovS (Fig. 5A). First is the finding that enhancing CovS activity through the addition of Mg^{2+} does not influence the already maximally repressed *hasA* and *scpC* genes in MGAS2221 (Fig. 5A) but does result in an ~15-fold decrease in *slo* mRNA abundance. Second is the

FIG 6 Legend (Continued)
mutant strain results in its binding only to promoters containing high-affinity CovR-binding sites, but not all high-affinity sites within a promoter will be filled, and hence, these genes will be only partially repressed. The virulence factor profile of *rocA*$^+$ strains is preferentially suited to promoting noninvasive infection (e.g., pharyngitis), while the virulence factor profile of *rocA* mutant strains is preferentially suited to promoting invasive infection (e.g., necrotizing fasciitis).

finding that the *hasA* and *scpC* genes, but not *slo*, are at least somewhat repressed by the addition of Mg^{2+} to strain 2221ΔrocA, consistent with the reduced amount of CovR~P that is generated in a *rocA* mutant in the presence of Mg^{2+} being rapidly sequestered by high-affinity binding sites located upstream of *hasA* and *scpC*. Thus, by having promoters that exhibit a range of affinities for CovR~P, GAS isolates are able to modulate gene expression in a nonuniform manner in response to CovRS-modulating stimuli.

As both M3 and M18 GAS isolates are *rocA* mutants and yet only M3 isolates are associated with causing particularly severe invasive infections, this implies that the *rocA* mutation is not sufficient for the association of M3 GAS with invasive disease. Consistent with this, we have shown that at least two other regulator-encoding genes, *rivR* and *fasC*, are also disrupted in M3 isolates (46), and we propose that it is the combined alteration in gene expression due to these mutations that pushes M3 GAS toward invasive disease hypervirulence. While serotype M3 and M18 GAS are the only known serotypes that are exclusively *rocA* mutant, individual isolates of other serotypes have also been identified as *rocA* mutant (22–25, 44, 47, 48). Data from several studies are consistent with *rocA* mutant strains being selected for from $rocA^+$ parental isolates, and that selection primarily occurs during invasive GAS infection (44, 47–49). This mirrors the more than 15 years worth of data concerning the selection of *covR* or *covS* mutant strains during invasive GAS infections (27–34, 50). The mutation of any one of the *rocA*, *covR*, and *covS* genes results in a virulence factor expression profile that promotes invasive disease, but undoubtedly there are important regulatory and virulence differences. The abundance of CovR~P appears to be a key correlate of invasive infection virulence, as there is an inverse correlation between levels of CovR~P (parental [wild type {WT}] > *rocA* mutant > *covS* mutant > *covR* mutant) and virulence (parental [WT] < *rocA* mutant < *covS* mutant < *covR* mutant) (30, 44). While not as extensively studied (32, 51, 52), we hypothesize that there is a positive correlation between the abundance of CovR~P and GAS virulence during noninvasive infections (parental [WT] > *rocA* mutant > *covS* mutant > *covR* mutant). As noninvasive infections represent the vast majority of GAS infections, it is tempting to speculate that this may explain why no GAS serotypes are exclusively *covR* or *covS* mutant, while some (M3 and M18) are exclusively *rocA* mutant. M3 and M18 isolates may be able to tolerate the reduced ability to cause noninvasive infections that comes with *rocA* mutation but not the greater levels of attenuation that would come with being *covS* or *covR* mutant.

In summary, we have expanded upon previous work by determining that RocA is an accessory protein to the CovRS two-component system. Our data are consistent with RocA enhancing the CovS-mediated phosphorylation of CovR, possibly through RocA-CovS interactions via their membrane-spanning domains. In a dose-dependent manner, RocA controls the abilities of LL-37 and Mg^{2+} to modulate CovS activity and hence modifies the ability of GAS to tailor gene expression during infection.

MATERIALS AND METHODS

Bacterial strains and growth conditions. The representative serotype M1 and M3 clinical GAS isolates MGAS2221 and MGAS10870, respectively, were used in this study (36, 46). Information about these strains and their derivatives is presented in Table 1. GAS isolates were grown in THY broth. Chloramphenicol (4 μg/ml), kanamycin (200 μg/ml), spectinomycin (150 μg/ml), LL-37 (100 nM), and $MgCl_2$ (50 mM) were added to the THY broth when needed. For standard cloning, *E. coli* DH5α cells were used. The *E. coli* cells were grown in LB broth with agitation at 37°C, with ampicillin (100 μg/ml), kanamycin (50 μg/ml), and chloramphenicol (20 μg/ml) added when needed.

Creation of plasmids pRocA-M1, pRocA-M3, and pRocA-M18. To facilitate the plasmid-based complementation of select *rocA* mutant strains, we created plasmid pRocA-M1, a plasmid that contains the functional *rocA* allele from serotype M1 GAS. The M1 *rocA* gene, along with its native promoter, was amplified by PCR (see Table S7 in the supplemental material for a list of primers used in this study) and cloned into the vector pDC123 (32, 53). Similar plasmids containing the serotype M3 or M18 *rocA* allele (plasmids pRocA-M3 and pRocA-M18, respectively) were also constructed. All the plasmids were sequence verified.

Creation of a library of pRocA-M1 derivatives expressing C-terminally truncated RocA proteins. To identify which domains of RocA are essential for regulatory activity, we created derivatives of pRocA-M1 in which deletions of increasing size were introduced at the 3′ end of the gene, resulting in the production of RocA proteins with C-terminal truncations of increasing size. The plasmids were

created by PCR (see Table S7 in the supplemental material), followed by Gibson assembly (New England BioLabs), and were verified by sequencing.

Hyaluronic acid capsule assays. Hyaluronic acid capsule assays were performed essentially as described previously (54). Briefly, GAS strains were grown in THY broth to mid-exponential phase. Aliquots of each culture were recovered, and the bacteria were pelleted by centrifugation. The bacterial pellets were resuspended in water, and serial dilutions were performed to ensure equivalent CFU numbers across strains. To remove the capsule, resuspended GAS cells were mixed with chloroform in a FastPrep machine before centrifuging to pellet the cellular debris. The aqueous phase was transferred to a clean tube, and the hyaluronic acid content was determined using an enzyme-linked immunosorbent assay (ELISA) kit (Corgenix) in accordance with the manufacturer's instructions.

Plate-based hyaluronidase assays. Plates containing 1% agarose, 1% bovine serum albumin (BSA), and 0.4 mg ml^{-1} of HA (sodium salt from *Streptococcus equi*) in 0.3 M sodium phosphate buffer (pH 5.3) were prepared as previously described (55). Wells (4 mm in diameter) were aseptically cut into the plates, and 100 μl of spent medium, taken from sterile-filtered THY broth cultures of each tested GAS strain grown to the exponential phase of growth (optical density at 600 nm [OD_{600}] = 0.5), were pipetted into separate wells. The plates were incubated overnight (18 to 20 h) at 37°C prior to flooding the plate with 2 M acetic acid. Clear zones were visualized against a background of opaque precipitated BSA conjugated to undigested HA, and their diameters were measured. Serial dilutions of hyaluronidase (MP Biochemicals, LLC) were used to enable construction of a standard curve to determine the concentration of hyaluronidase in the spent medium. Biological replicates of each GAS strain were assayed in duplicate.

Lancefield bactericidal assays. Bactericidal assays were performed essentially as previously described (24). Briefly, cultures of the three GAS strains to be compared were grown to the early exponential phase of growth (corresponding to an OD_{600} of 0.15 to 0.2). Upon reaching the correct OD, each sample was diluted to $\sim 1 \times 10^4$ CFU/ml using sterile phosphate-buffered saline (PBS). Subsequently, 50 μl of the diluted GAS cultures was added to individual aliquots of nonimmune heparinized whole human blood and incubated by end-over-end rotation for 3 h at 37°C. At the same time, 50 μl of the PBS-diluted GAS cultures was plated onto blood agar plates to enable accurate calculation of the initial inocula. Following incubation, 50 μl of the blood-GAS mixtures was plated onto blood agar directly and also after performing 1:10 and 1:100 dilutions with PBS. All the plated samples were incubated overnight at 37°C with 5% carbon dioxide. Colony counts of each strain were categorized and tabulated for average survival in human blood.

Total RNA isolation from GAS. Total RNA was isolated from select GAS strains as previously described (30). Briefly, GAS strains were grown to the mid-exponential phase of growth (corresponding to an OD_{600} of 0.5) in THY broth. One volume of GAS culture was subsequently added to 2 volumes of RNAprotect bacterial reagent (Qiagen) and incubated at room temperature for 5 min. Following centrifugation at 5,000 $\times$ *g* for 10 min at 4°C, the bacterial pellets were snap-frozen in liquid nitrogen and stored at −80°C until ready for use. The bacterial cells were processed for RNA isolation using a mechanical lysis method in conjunction with the RNeasy minikit (Qiagen). Contaminating DNA was removed by three 40-min treatments with Turbo-DNase-free (Life Technologies). The quality and quantity of the isolated RNA were assessed by using a Bioanalyzer 2100 system (Agilent Technologies).

RNA-seq analysis. THY broth cultures of the tested GAS strains were grown to the exponential phase of growth (OD_{600} = 0.5). Total RNA was isolated, and rRNAs, which represent ~96% of the total RNA, were depleted using the Ribo-Zero Gram-positive rRNA removal kit (Epicentre). The rRNA-depleted RNA was then used to generate cDNA libraries for sequencing according to a previously described protocol using a ScriptSeq kit (Epicentre) (56). Briefly, RNA was fragmented, cDNA was synthesized using random hexamers containing a 5′ tagging sequence, the RNA was hydrolyzed, and the cDNA was tagged at the 3′ end. A limited number of PCR cycles (*n* = 12 to 14) were used to amplify the libraries via the 5′ and 3′ tags (the libraries were barcoded using different primers), and the libraries were size selected (170 to 300 bp). The size-selected and barcoded libraries were run on an Illumina flow cell using a HiSeq (Fig. 2) or MiSeq (see Fig. S2 in the supplemental material) instrument. Data were analyzed using CLC Genomics Workbench and normalized to the overall sequencing depth using total mapped read data. Statistical significance was tested using Kal's Z test with a false-discovery rate correction (24).

Quantitative RT-PCR analysis. Total mRNA samples were isolated and converted into cDNA using the reverse transcriptase Superscript III (Life Technologies). The generated cDNA was analyzed via TaqMan-based quantitative RT-PCR analysis using a CFX Connect Real-Time System (Bio-Rad). TaqMan primers and probes for genes of interest, and the internal control gene *proS*, are shown in Table S7 in the supplemental material. Transcript levels were determined using the $\Delta\Delta C_T$ method.

Accession number(s). The RNA-seq data have been deposited in the Gene Expression Omnibus (GEO) database at the National Center for Biotechnology Information (http://www.ncbi.nlm.nih.gov/geo) and are accessible through accession numbers GSE97325 and GSE101893.

SUPPLEMENTAL MATERIAL

Supplemental material for this article may be found at https://doi.org/10.1128/IAI.00274-17.

SUPPLEMENTAL FILE 1, PDF file, 1.4 MB.

ACKNOWLEDGMENTS

Funding for this research was through grant 16GRNT27650010 from the American Heart Association (AHA) (to P.S.). We thank Mick Hitchcock for his support of J.L.D., who is a Hitchcock Scholar.

REFERENCES

1. Heithoff DM, Shimp WR, House JK, Xie Y, Weimer BC, Sinsheimer RL, Mahan MJ. 2012. Intraspecies variation in the emergence of hyperinfectious bacterial strains in nature. PLoS Pathog 8:e1002647. https://doi.org/10.1371/journal.ppat.1002647.
2. Willems RJ, Hanage WP, Bessen DE, Feil EJ. 2011. Population biology of Gram-positive pathogens: high-risk clones for dissemination of antibiotic resistance. FEMS Microbiol Rev 35:872–900. https://doi.org/10.1111/j.1574-6976.2011.00284.x.
3. Gomes TA, Elias WP, Scaletsky IC, Guth BE, Rodrigues JF, Piazza RM, Ferreira LC, Martinez MB. 2016. Diarrheagenic Escherichia coli. Braz J Microbiol 47(Suppl 1):3–30. https://doi.org/10.1016/j.bjm.2016.10.015.
4. Chen Y, Gao J, Zhang H, Ying C. 2017. Spread of the blaOXA-23-containing Tn2008 in carbapenem-resistant Acinetobacter baumannii isolates grouped in CC92 from China. Front Microbiol 8:163. https://doi.org/10.3389/fmicb.2017.00163.
5. Nigro SJ, Holt KE, Pickard D, Hall RM. 2015. Carbapenem and amikacin resistance on a large conjugative Acinetobacter baumannii plasmid. J Antimicrob Chemother 70:1259–1261. https://doi.org/10.1093/jac/dkv102.
6. Sarkar P, Sumby P. 2017. Regulatory gene mutation: a driving force behind group A Streptococcus strain- and serotype-specific variation. Mol Microbiol 103:576–589. https://doi.org/10.1111/mmi.13584.
7. Cheung GY, Wang R, Khan BA, Sturdevant DE, Otto M. 2011. Role of the accessory gene regulator agr in community-associated methicillin-resistant Staphylococcus aureus pathogenesis. Infect Immun 79:1927–1935. https://doi.org/10.1128/IAI.00046-11.
8. Uhlemann AC, Otto M, Lowy FD, DeLeo FR. 2014. Evolution of community- and healthcare-associated methicillin-resistant Staphylococcus aureus. Infect Genet Evol 21:563–574. https://doi.org/10.1016/j.meegid.2013.04.030.
9. Novick RP. 2003. Autoinduction and signal transduction in the regulation of staphylococcal virulence. Mol Microbiol 48:1429–1449. https://doi.org/10.1046/j.1365-2958.2003.03526.x.
10. Aracil B, Slack M, Perez-Vazquez M, Roman F, Ramsay M, Campos J. 2006. Molecular epidemiology of Haemophilus influenzae type b causing vaccine failures in the United Kingdom. J Clin Microbiol 44:1645–1649. https://doi.org/10.1128/JCM.44.5.1645-1649.2006.
11. Croucher NJ, Harris SR, Fraser C, Quail MA, Burton J, van der Linden M, McGee L, von Gottberg A, Song JH, Ko KS, Pichon B, Baker S, Parry CM, Lambertsen LM, Shahinas D, Pillai DR, Mitchell TJ, Dougan G, Tomasz A, Klugman KP, Parkhill J, Hanage WP, Bentley SD. 2011. Rapid pneumococcal evolution in response to clinical interventions. Science 331:430–434. https://doi.org/10.1126/science.1198545.
12. Tientcheu LD, Koch A, Ndengane M, Andoseh G, Kampmann B, Wilkinson RJ. 2017. Immunological consequences of strain variation within the Mycobacterium tuberculosis complex. Eur J Immunol 47:432–445. https://doi.org/10.1002/eji.201646562.
13. Cunningham MW. 2008. Pathogenesis of group A streptococcal infections and their sequelae. Adv Exp Med Biol 609:29–42. https://doi.org/10.1007/978-0-387-73960-1_3.
14. Martin WJ, Steer AC, Smeesters PR, Keeble J, Inouye M, Carapetis J, Wicks IP. 2015. Post-infectious group A streptococcal autoimmune syndromes and the heart. Autoimmun Rev 14:710–725. https://doi.org/10.1016/j.autrev.2015.04.005.
15. Brouwer S, Barnett TC, Rivera-Hernandez T, Rohde M, Walker MJ. 2016. Streptococcus pyogenes adhesion and colonization. FEBS Lett 590:3739–3757. https://doi.org/10.1002/1873-3468.12254.
16. Hynes W, Sloan M. 2016. Secreted extracellular virulence factors, p 405–444. *In* Ferretti JJ, Stevens DL, Fischetti VA (ed), Streptococcus pyogenes: basic biology to clinical manifestations. University of Oklahoma Health Sciences Center, Oklahoma City, OK.
17. Ichikawa M, Minami M, Isaka M, Tatsuno I, Hasegawa T. 2011. Analysis of two-component sensor proteins involved in the response to acid stimuli in Streptococcus pyogenes. Microbiology 157:3187–3194. https://doi.org/10.1099/mic.0.050534-0.
18. Vega LA, Malke H, McIver KS. 2016. Virulence-related transcriptional regulators of Streptococcus pyogenes, p 337–404. *In* Ferretti JJ, Stevens DL, Fischetti VA (ed), Streptococcus pyogenes: basic biology to clinical manifestations. University of Oklahoma Health Sciences Center, Oklahoma City, OK.
19. Danger JL, Makthal N, Kumaraswami M, Sumby P. 2015. The FasX small regulatory RNA negatively regulates the expression of two fibronectin-binding proteins in group A Streptococcus. J Bacteriol 197:3720–3730. https://doi.org/10.1128/JB.00530-15.
20. Johnson DR, Stevens DL, Kaplan EL. 1992. Epidemiologic analysis of group A streptococcal serotypes associated with severe systemic infections, rheumatic fever, or uncomplicated pharyngitis. J Infect Dis 166:374–382. https://doi.org/10.1093/infdis/166.2.374.
21. Smoot JC, Barbian KD, Van Gompel JJ, Smoot LM, Chaussee MS, Sylva GL, Sturdevant DE, Ricklefs SM, Porcella SF, Parkins LD, Beres SB, Campbell DS, Smith TM, Zhang Q, Kapur V, Daly JA, Veasy LG, Musser JM. 2002. Genome sequence and comparative microarray analysis of serotype M18 group A Streptococcus strains associated with acute rheumatic fever outbreaks. Proc Natl Acad Sci U S A 99:4668–4673. https://doi.org/10.1073/pnas.062526099.
22. Lynskey NN, Goulding D, Gierula M, Turner CE, Dougan G, Edwards RJ, Sriskandan S. 2013. RocA truncation underpins hyper-encapsulation, carriage longevity and transmissibility of serotype M18 group A streptococci. PLoS Pathog 9:e1003842. https://doi.org/10.1371/journal.ppat.1003842.
23. Lynskey NN, Turner CE, Heng LS, Sriskandan S. 2015. A truncation in the regulator RocA underlies heightened capsule expression in serotype M3 group A streptococci. Infect Immun 83:1732–1733. https://doi.org/10.1128/IAI.02892-14.
24. Miller EW, Danger JL, Ramalinga AB, Horstmann N, Shelburne SA, Sumby P. 2015. Regulatory rewiring confers serotype-specific hyper-virulence in the human pathogen group A Streptococcus. Mol Microbiol 98:473–489. https://doi.org/10.1111/mmi.13136.
25. Miller EW, Pflughoeft KJ, Sumby P. 2015. Reply to "A truncation in the regulator RocA underlies heightened capsule expression in serotype M3 group A streptococci". Infect Immun 83:1734. https://doi.org/10.1128/IAI.03162-14.
26. Biswas I, Scott JR. 2003. Identification of rocA, a positive regulator of covR expression in the group A streptococcus. J Bacteriol 185:3081–3090. https://doi.org/10.1128/JB.185.10.3081-3090.2003.
27. Levin JC, Wessels MR. 1998. Identification of csrR/csrS, a genetic locus that regulates hyaluronic acid capsule synthesis in group A Streptococcus. Mol Microbiol 30:209–219. https://doi.org/10.1046/j.1365-2958.1998.01057.x.
28. Federle MJ, McIver KS, Scott JR. 1999. A response regulator that represses transcription of several virulence operons in the group A streptococcus. J Bacteriol 181:3649–3657.
29. Graham MR, Smoot LM, Migliaccio CA, Virtaneva K, Sturdevant DE, Porcella SF, Federle MJ, Adams GJ, Scott JR, Musser JM. 2002. Virulence control in group A Streptococcus by a two-component gene regulatory system: global expression profiling and in vivo infection modeling. Proc Natl Acad Sci U S A 99:13855–13860. https://doi.org/10.1073/pnas.202353699.
30. Sumby P, Whitney AR, Graviss EA, DeLeo FR, Musser JM. 2006. Genome-wide analysis of group A streptococci reveals a mutation that modulates global phenotype and disease specificity. PLoS Pathog 2:e5. https://doi.org/10.1371/journal.ppat.0020005.
31. Cole JN, McArthur JD, McKay FC, Sanderson-Smith ML, Cork AJ, Ranson M, Rohde M, Itzek A, Sun H, Ginsburg D, Kotb M, Nizet V, Chhatwal GS, Walker MJ. 2006. Trigger for group A streptococcal M1T1 invasive disease. FASEB J 20:1745–1747. https://doi.org/10.1096/fj.06-5804fje.
32. Trevino J, Perez N, Ramirez-Pena E, Liu Z, Shelburne SA, III, Musser JM, Sumby P. 2009. CovS simultaneously activates and inhibits the CovR-mediated repression of distinct subsets of group A Streptococcus viru-

lence factor-encoding genes. Infect Immun 77:3141–3149. https://doi.org/10.1128/IAI.01560-08.
33. Li J, Liu G, Feng W, Zhou Y, Liu M, Wiley JA, Lei B. 2014. Neutrophils select hypervirulent CovRS mutants of M1T1 group A Streptococcus during subcutaneous infection of mice. Infect Immun 82:1579–1590. https://doi.org/10.1128/IAI.01458-13.
34. Horstmann N, Sahasrabhojane P, Saldana M, Ajami NJ, Flores AR, Sumby P, Liu CG, Yao H, Su X, Thompson E, Shelburne SA. 2015. Characterization of the effect of the histidine kinase CovS on response regulator phosphorylation in group A Streptococcus. Infect Immun 83:1068–1077. https://doi.org/10.1128/IAI.02659-14.
35. Velarde JJ, Ashbaugh M, Wessels MR. 2014. The human antimicrobial peptide LL-37 binds directly to CsrS, a sensor histidine kinase of group A Streptococcus, to activate expression of virulence factors. J Biol Chem 289:36315–36324. https://doi.org/10.1074/jbc.M114.605394.
36. Sumby P, Porcella SF, Madrigal AG, Barbian KD, Virtaneva K, Ricklefs SM, Sturdevant DE, Graham MR, Vuopio-Varkila J, Hoe NP, Musser JM. 2005. Evolutionary origin and emergence of a highly successful clone of serotype M1 group A Streptococcus involved multiple horizontal gene transfer events. J Infect Dis 192:771–782. https://doi.org/10.1086/432514.
37. Kal AJ, van Zonneveld AJ, Benes V, van den Berg M, Koerkamp MG, Albermann K, Strack N, Ruijter JM, Richter A, Dujon B, Ansorge W, Tabak HF. 1999. Dynamics of gene expression revealed by comparison of serial analysis of gene expression transcript profiles from yeast grown on two different carbon sources. Mol Biol Cell 10:1859–1872. https://doi.org/10.1091/mbc.10.6.1859.
38. Gryllos I, Tran-Winkler HJ, Cheng MF, Chung H, Bolcome R, III, Lu W, Lehrer RI, Wessels MR. 2008. Induction of group A Streptococcus virulence by a human antimicrobial peptide. Proc Natl Acad Sci U S A 105:16755–16760. https://doi.org/10.1073/pnas.0803815105.
39. Gryllos I, Grifantini R, Colaprico A, Jiang S, Deforce E, Hakansson A, Telford JL, Grandi G, Wessels MR. 2007. Mg(2+) signalling defines the group A streptococcal CsrRS (CovRS) regulon. Mol Microbiol 65:671–683. https://doi.org/10.1111/j.1365-2958.2007.05818.x.
40. Jung K, Fried L, Behr S, Heermann R. 2012. Histidine kinases and response regulators in networks. Curr Opin Microbiol 15:118–124. https://doi.org/10.1016/j.mib.2011.11.009.
41. Buelow DR, Raivio TL. 2010. Three (and more) component regulatory systems—auxiliary regulators of bacterial histidine kinases. Mol Microbiol 75:547–566. https://doi.org/10.1111/j.1365-2958.2009.06982.x.
42. Tschauner K, Hornschemeyer P, Muller VS, Hunke S. 2014. Dynamic interaction between the CpxA sensor kinase and the periplasmic accessory protein CpxP mediates signal recognition in E. coli. PLoS One 9:e107383. https://doi.org/10.1371/journal.pone.0107383.
43. Surmann K, Cudic E, Hammer E, Hunke S. 2016. Molecular and proteome analyses highlight the importance of the Cpx envelope stress system for acid stress and cell wall stability in Escherichia coli. Microbiology Open 5:582–596. https://doi.org/10.1002/mbo3.353.
44. Feng W, Minor D, Liu M, Li J, Ishaq SL, Yeoman C, Lei B. 2017. Null mutations of group A Streptococcus orphan kinase RocA: selection in mouse infection and comparison with CovS mutations in alteration of in vitro and in vivo protease SpeB expression and virulence. Infect Immun 85:e00790-16. https://doi.org/10.1128/IAI.00790-16.
45. Churchward G, Bates C, Gusa AA, Stringer V, Scott JR. 2009. Regulation of streptokinase expression by CovR/S in Streptococcus pyogenes: CovR acts through a single high-affinity binding site. Microbiology 155:566–575. https://doi.org/10.1099/mic.0.024620-0.
46. Beres SB, Sylva GL, Sturdevant DE, Granville CN, Liu M, Ricklefs SM, Whitney AR, Parkins LD, Hoe NP, Adams GJ, Low DE, DeLeo FR, McGeer A, Musser JM. 2004. Genome-wide molecular dissection of serotype M3 group A Streptococcus strains causing two epidemics of invasive infections. Proc Natl Acad Sci U S A 101:11833–11838. https://doi.org/10.1073/pnas.0404163101.
47. Yoshida H, Ishigaki Y, Takizawa A, Moro K, Kishi Y, Takahashi T, Matsui H. 2015. Comparative genomics of the mucoid and nonmucoid strains of Streptococcus pyogenes, isolated from the same patient with streptococcal meningitis. Genome Announc 3:e00221-15. https://doi.org/10.1128/genomeA.00221-15.
48. Zhu L, Olsen RJ, Horstmann N, Shelburne SA, Fan J, Hu Y, Musser JM. 2016. Intergenic variable-number tandem-repeat polymorphism upstream of rocA alters toxin production and enhances virulence in Streptococcus pyogenes. Infect Immun 84:2086–2093. https://doi.org/10.1128/IAI.00258-16.
49. Ikebe T, Matsumura T, Nihonmatsu H, Ohya H, Okuno R, Mitsui C, Kawahara R, Kameyama M, Sasaki M, Shimada N, Ato M, Ohnishi M. 2016. Spontaneous mutations in Streptococcus pyogenes isolates from streptococcal toxic shock syndrome patients play roles in virulence. Sci Rep 6:28761. https://doi.org/10.1038/srep28761.
50. Engleberg NC, Heath A, Miller A, Rivera C, DiRita VJ. 2001. Spontaneous mutations in the CsrRS two-component regulatory system of Streptococcus pyogenes result in enhanced virulence in a murine model of skin and soft tissue infection. J Infect Dis 183:1043–1054. https://doi.org/10.1086/319291.
51. Hollands A, Pence MA, Timmer AM, Osvath SR, Turnbull L, Whitchurch CB, Walker MJ, Nizet V. 2010. Genetic switch to hypervirulence reduces colonization phenotypes of the globally disseminated group A streptococcus M1T1 clone. J Infect Dis 202:11–19. https://doi.org/10.1086/653124.
52. Alam FM, Turner CE, Smith K, Wiles S, Sriskandan S. 2013. Inactivation of the CovR/S virulence regulator impairs infection in an improved murine model of Streptococcus pyogenes naso-pharyngeal infection. PLoS One 8:e61655. https://doi.org/10.1371/journal.pone.0061655.
53. Chaffin DO, Rubens CE. 1998. Blue/white screening of recombinant plasmids in Gram-positive bacteria by interruption of alkaline phosphatase gene (phoZ) expression. Gene 219:91–99. https://doi.org/10.1016/S0378-1119(98)00396-5.
54. Trevino J, Liu Z, Cao TN, Ramirez-Pena E, Sumby P. 2013. RivR is a negative regulator of virulence factor expression in group A Streptococcus. Infect Immun 81:364–372. https://doi.org/10.1128/IAI.00703-12.
55. Steiner B, Cruce D. 1992. A zymographic assay for detection of hyaluronidase activity on polyacrylamide gels and its application to enzymatic activity found in bacteria. Anal Biochem 200:405–410. https://doi.org/10.1016/0003-2697(92)90487-R.
56. McClure R, Balasubramanian D, Sun Y, Bobrovskyy M, Sumby P, Genco CA, Vanderpool CK, Tjaden B. 2013. Computational analysis of bacterial RNA-Seq data. Nucleic Acids Res 41:e140. https://doi.org/10.1093/nar/gkt444.
57. Cao TN, Liu Z, Cao TH, Pflughoeft KJ, Treviño J, Danger JL, Beres SB, Musser JM, Sumby P. 2014. Natural disruption of two regulatory networks in serotype M3 group A Streptococcus isolates contributes to the virulence factor profile of this hypervirulent serotype. Infect Immun 82:1744–1754. https://doi.org/10.1128/IAI.01639-13.